5.7 A 256×256 40nm/90nm CMOS 3D-Stacked 120dB-Dynamic-Range Reconfigurable Time-Resolved SPAD Imager

Robert K. Henderson[1], Nick Johnston[1], Sam W. Hutchings[1], Istvan Gyongy[1], Tarek Al Abbas[1], Neale Dutton[2], Max Tyler[3], Susan Chan[3], Jonathan Leach[3]

[1]University of Edinburgh, Edinburgh, United Kingdom
[2]STMicroelectronics, Edinburgh, United Kingdom
[3]Heriot-Watt University, Edinburgh, United Kingdom

Light Detection and Ranging (LIDAR) applications pose extremely challenging dynamic range (DR) requirements on optical time-of-flight (ToF) receivers due to laser returns affected by the inverse square law over 2-3 decades of distance, diverse target reflectivity, and high solar background [1]. Integrated CMOS SPADs have a native DR exceeding 140dB, typically extending from the noise floor of few cps to 100's Mcps peak rate. To deliver this DR to downstream DSP, large SPAD time-resolved imaging arrays must count and time billions of single photon events per second demanding massively parallel on-chip pixel processing to achieve practical I/O power consumption and data rates. Hybrid Cu-Cu bonding offers a mass-manufacturable platform to implement these sensors by providing high-fill-factor SPADs optimised for NIR stacked on dense nanoscale digital processors [2]. Stacked sensor architectures involving pixel-level histogramming, on-chip peak detection and TDC/processor resource sharing are now being investigated [3-5].

This paper presents a large imaging array of compact, reconfigurable SPAD time-resolved pixels in a 3D stacked 40nm/90nm CMOS technology. Figure 5.7.1a shows the chip organisation, 8 I/O pads generate a modest 31.6Mbps of pixel data at the targeted 30fps (a maximum of 800Mbps at 760fps) via either a rolling or global shutter readout scheme. A uniform top-tier BSI matrix of 256×256 pwell/deep-nwell SPADs at 9.2µm pitch with 51% fill-factor and median dark count rate of 20cps at 1.5V excess bias. In the bottom-tier a 64×64 matrix of modular photon processors at 38.4µm pitch is integrated in 40nm CMOS technology with ~40M transistors. Figure 5.7.1b shows an interface circuit that is agnostic to the SPAD polarity for compatibility to future detector generations. External global *Vqp* and *Vqn* voltages and the *Invert* signal allow selection of either NMOS or PMOS quench transistors and time gating. An enable SRAM allows masking of noisy detectors. Two time-gated paths are implemented for photon counting or photon timing as *SPAD(k)* and *Start(k)* respectively. For photon counting, under control of *ToggleEn* signal, the *Start(k)* signal can encode photons on both rising and falling edges or transition once to report the first photon in an exposure time. For photon timing, it is possible to count STOP pulses by re-using the same path to generate macro-time stamps.

The 16 *Start(k)* toggling outputs are mixed via a XOR tree to a single sequence *PhotonEdges* that is passed to the multi-event TDC (METDC). In addition, *PhotonEdges* is processed by a multi-photon trigger circuit [5], which continually counts photons from the first rising edge received in a laser cycle. A threshold of 1, 2, 4, 8 photons occurring within a 1-to-10ns delay time (adjustable by current starving voltage *Vndelay*) generates an output trigger to start the gated ring oscillator (GRO). This circuit saves power by only activating the GRO if there is a highly correlated burst of photons likely to belong to a laser return while suppressing uncorrelated background light. The signal *Qtrig* enables a qualified trigger as the delayed first photon in the burst if the threshold has been met. In addition, a toggling trigger sequence can be generated on multiple bursts for use in the METDC. The METDC is based on the architecture presented in [6] operating with a shift-register delay chain to allow adjustable time bin resolution. This architecture allows time digitisation of up to 16 photons per laser cycle, or 1 photon per SPAD per laser cycle. Time bin resolution is set over a range 0.56ns to 560ns by *TDCclk* by selection of a divided phase of the GRO (Fig. 5.7.2b). This clock starts only on the first trigger (single or multi-photon) for power saving. The 14b GRO TDC is adjustable by the *Vddro* voltage over a full-scale range of 560ns to 1.6µs for a 35-to-100ps LSB resolution, matched to common automotive LIDAR ranges. Alternatively, for longer distance range *TDCclk* can connected to a lower frequency external clock *ExtClk*.

Finally, the 16×14b ripple counter array and mode multiplexer allow the sensor to operate in three main imaging modalities: (1) global-shutter (GS) single photon counting (SPC) for gated intensity imaging, and time-resolved imaging via (2) triggered timestamping or (3) multi-event coarse histogramming.

For SPC mode, the 16 counters receive inputs from the 16 *SPAD(k)* signals capturing full 256×256 image resolution with 16k photon full-well capacity (84dB DR). GS-HDR modes are realised by chaining the counters into 8×28b whilst binning groups of 4 SPADs allowing 256M photons per SPAD to be counted in an exposure period with a 64×264 spatial resolution. Figure 5.7.3a-d shows a HDR scene taken in 1k and 100 klux illumination at 30fps showing a 14b 1klux image, rollover of the 14b counters at 100klux and a tone-mapped unsaturated 100klux 28b image. The GS capture is parasitic light insensitive as the BSI sensor is all-digital. A DR of 120dB is seen in the photon transfer curve in Fig. 5.7.3c with peak count rates of 200Mcps/SPAD or 13Tcps for the whole array. We now achieve full native SPAD dynamic range is available in a video-rate image sensor.

For the two time-resolved modes, the 16 METDC bin outputs *TDC(k)* are directed to the counters, capturing 262k triggers (single or multiphoton) per histogram before saturation. The mode multiplexer can also be configured to an HDR METDC mode by chaining pairs of 14b counters to 28b with a reduced number of time bins. Sparing activation of the 14b GRO TDC through the multiphoton trigger is economic in both power consumption and I/O bandwidth, as these resources are not expended on background photon detections. Figure 5.7.4a shows histograms generated with 1 and 2 photon trigger levels showing considerable background rejection and sharper peak. Figure 5.7.4c shows a TDC nonlinearity of ±10cm over a 50m range. These data were obtained with a 671nm Picoquant pulsed laser coupled into a 100µm multimode fiber and passed through a 15mm lens to flood illuminate the scene. The pulse duration of the laser was ~100ps, the repetition rate was 1.9MHz, and after the fibre and imaging lens, the laser power was measured to be 1.8mW. Figure 5.7.4d shows the impulse response function of 240ps FWHM. Figure 5.7.5a and b detail two-step timings to allow the coarse METDC mode to be applied to generate 3D video images at >50m distances. The first timing approach operates the 16 bins over the full distance range with a *ExtClk* synchronised to 16 times the laser rate set by the round trip time. A first exposure is taken to determine the four MSBs of the target range. In a second exposure, the laser rate is increased by 16× and the in-pixel GRO *TDCclk* generates the METDC clock. This determines the next four LSBs of the target range but aliases the background noise. The second timing approach to achieve the same disambiguation is to apply the multiphoton triggered mode with a high threshold to timestamp the laser return. In this case, power consumption and jitter of the GRO can be reduced by operating with a STOP clock at 16× laser repetition rate and using the macro-time stamp feature to count STOP cycles. Figure 5.7.5c shows distance accuracy improved over that expected from the 560ps bin size by spreading the pulse energy over bins and performing centroiding around the peak. In this operating condition, the sensor consumes 77.6mW including SPAD, GRO and digital core, considerably lower than TDC array approaches. Figure 5.7.6 shows a table of comparison of this sensor.

Acknowledgements:
This work was supported by the Engineering and Physical Sciences Research Council through the Quantum Hub in Quantum Enhanced Imaging EP/M01326X/1. We are grateful to STMicroelectronics and the ENIAC-POLIS project for chip fabrication. The EPSRC CDT in Intelligent Sensing and Measurement, Grant Number EP/L016753/1 supported Sam Hutchings' work.

References:
[1] C. Niclass, et al., "A 100-m Range 10-Frame/s 340 x 96-Pixel Time-of-Flight Depth Sensor in 0.18-µm CMOS," *IEEE JSSC*, vol. 48, no. 2, pp. 559-572, Feb. 2013.
[2] T. A. Abbas, et al., "Backside Illuminated SPAD Image Sensor with 7.83µm Pitch in 3D-Stacked CMOS Technology," *IEDM*, pp. 8.1.1-8.1.4, 2016.
[3] S. Lindner, et al., "A 252 × 144 SPAD Pixel FLASH LiDAR with 1728 Dual-clock 48.8 ps TDCs, Integrated Histogramming and 14.9-to-1 Compression in 180nm CMOS Technology", *IEEE Symp. VLSI Circuits*, pp. 69-70, 2018.
[4] A. Ximenes, et al., "A 256×256 45/65nm 3D-Stacked SPAD-Based Direct TOF Image Sensor for LiDAR Applications with Optical Polar Modulation for up to 18.6dB Interference Suppression", *ISSCC Dig. Tech. Papers*, pp. 96-98, Feb. 2018.
[5] M. Perenzoni, et al., "A 64 x 64-Pixels Digital Silicon Photomultiplier Direct TOF Sensor with 100-MPhotons/s/pixel Background Rejection and Imaging/Altimeter Mode with 0.14% Precision Up To 6 km for Spacecraft Navigation and Landing," *IEEE JSSC*, vol. 52, no. 1, pp. 151-160, Jan. 2017.
[6] N.A.W. Dutton, et al., "11.5 A Time-Correlated Single-Photon-Counting Sensor with 14GS/S Histogramming Time-to-Digital Converter," *ISSCC Dig. Tech. Papers*, Feb. 2015.

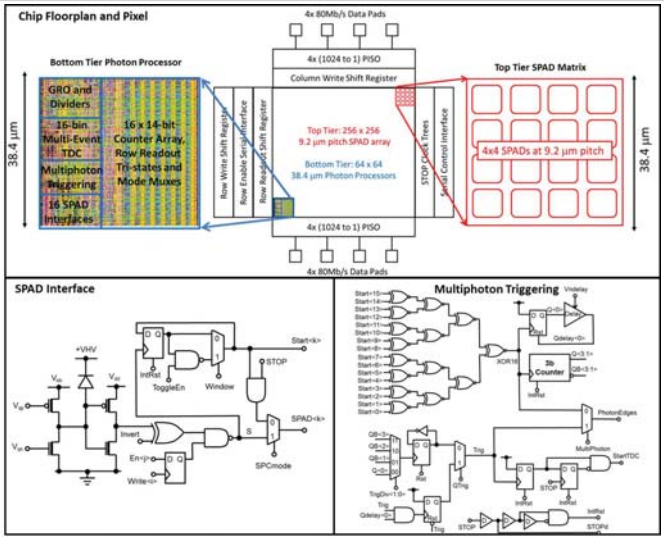

Figure 5.7.1: (a) Chip floorplan and pixel organisation, (b) SPAD interface, and (c) multiphoton triggering circuit.

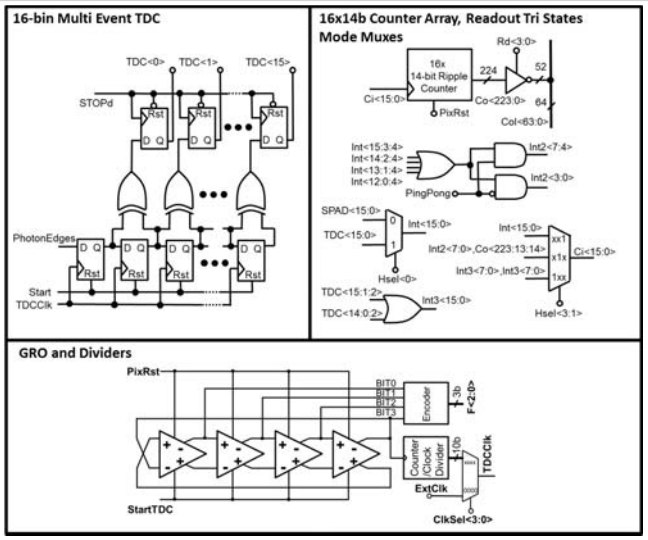

Figure 5.7.2: (a) 16-bin multi-event TDC; (b) 16×14b counter array, readout tri-states and mode mux; (c) GRO and dividers.

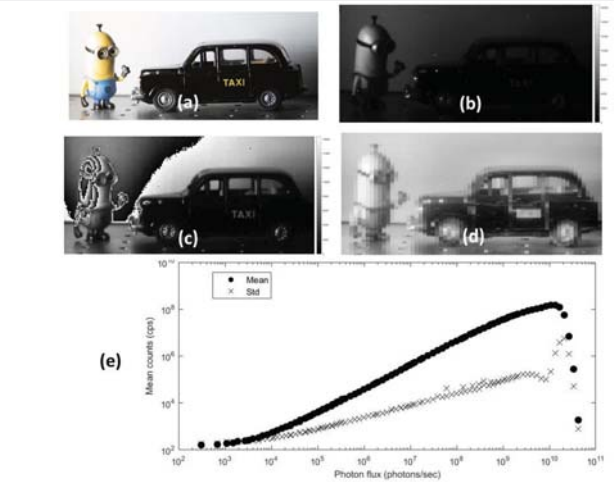

Figure 5.7.3: SPC mode: (a) side-illuminated scene with Nikon camera; (b) 1klux illumination 14b image; (c) 100klux illumination 14b code roll-over image; (d) 100klux illumination 28b image with 4× pixel binning; and (e) photon transfer curve showing 120dB DR in 28b mode.

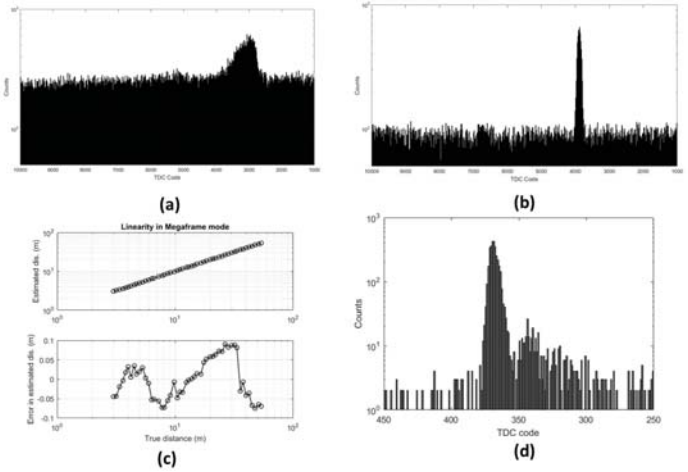

Figure 5.7.4: Multiphoton triggering mode: (a) reflected laser pulse in 1klux ambient; (b) with multiphoton triggering enabled with 2 threshold; (c) linearity sweep over 50m; (d) impulse response function.

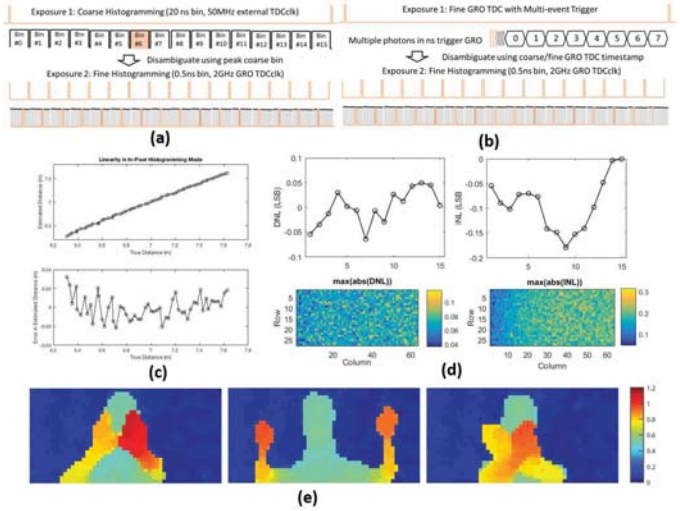

Figure 5.7.5: In-pixel histogramming mode: (a),(b) two-step timing schemes for LIDAR; (c) distance sweep over 1.6m; (d) histogram bin uniformity over full array; (e) 3 images from a 30fps movie taken at 50m.

Parameters	Units	This Work	[3]	[4]	[5]	[1]
			Sensor			
CMOS Technology	-	**40nm/90nm**	180nm	45nm/65nm	150nm	180nm
Pixel Array	-	**256x256/64x64**	252x144	16x8	64x64	16x1/32x1
Pixel Pitch	µm	**9.2/38.4**	28.5	19.8	60	21
Fill-factor	%	**51**	28	31.3/50.6	26.5	70
Median DCR@Vex	cps	**20@1.5V**	195 @5V	5.3k@2.5V	6.8k@3V	2.65k@NA
TDC depth	bits	**14/4**	12	14	16/15	12
TDC resolution	ps	**35/560**	48.8	60-320	250-20000	208
TDC area	µm²	**130/150**	4200	550	NA	NA
TDC number	-	**4096**	1728	1	4096	64
TDC linearity DNL/INL	LSB	**+0.05/-0.05 +0.1/-0.08**	+0.6/-0.48 +0.89/-1.67	+0.8/-0.7 +3.4/-0.8	+1.2/-1 +4.8/-3.2	+0.15/-0.17 +0.32/-0.56
			LIDAR Measurement			
Image resolution	-	**64x64**	252x144	256x256	64x64	202x96
Laser projection	-	**Flash**	Flash	Scanning	Flash	Scanning
Wavelength	nm	**671**	637	532	470	870
Repetition rate	MHz	**1.9**	40	1	NA	0.133
Mean illumination power	mW	**1.8**	2	6	NA	21
PDP@ illumination wavelength@Vex	%	**23@3V**	33.7@5V	21@2.5V	20@3V	NA
Max distance	m	**50**	50	150-430	367-5862	128
Imaging range	m	**50**	0.7	4.5	NA	100
FOV	deg.	**1.2x1.2**	40x20	NA	NA	
Accuracy	m(%)	**0.17(0.34)**	0.088(0.17)	0.07(0.3)	1.5(0.37)	11(0.11)
Background light	-	**1klux**	dark	NA	100M/pix/s	70 klux
Target reflectivity	-	**white**	white	white	NA	9%
Power consumption	mW	**77.6**	2540	NA	93.5	530

Figure 5.7.6: Table of comparison.

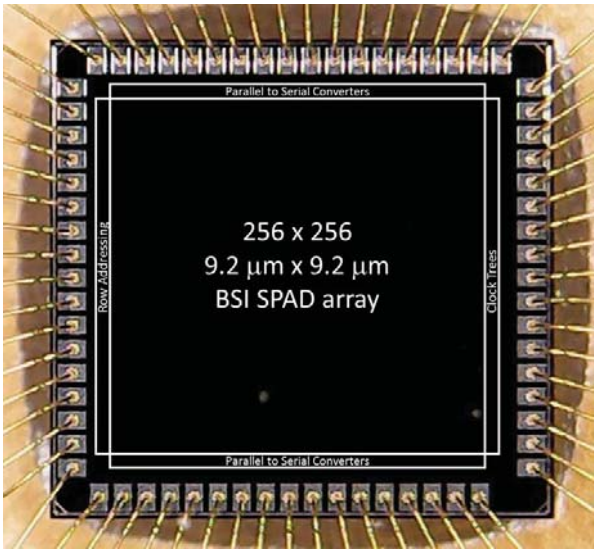

Figure 5.7.7: Chip micrograph.

978-1-5386-8531-0/19/$31.00